Journal of Magnetism and Magnetic Materials 541 (2022) 168484

Contents lists available at ScienceDirect

Journal of Magnetism and Magnetic Materials

journal homepage: www.elsevier.com/locate/jmmm

Research articles

# Ferroelectric-Ferromagnetic Heterostructures based on Sodium Substituted Lanthanum Manganite Thin films deposited on PMN-PT substrate by Pulsed Laser Deposition

N. Sethulakshmi [a,1], Lalitha K.V. [b,2], Senoy Thomas [a], G. Srinivasan [c], M.R. Anantharaman [a,*]

[a] Department of Physics, Cochin University of Science and Technology, Cochin 682 022, India
[b] Department of Materials Engineering, Indian Institute of Science, Bangalore 560 012, India
[c] Department of Physics, Oakland University, Rochester, MI 48309-4401, USA

ARTICLE INFO

*Keywords:*
Lanthanum manganites
Manganite thin films
PMN-PT LNMO
Ferroelectric-ferromagnetic heterostructure

ABSTRACT

Phase pure targets of sodium substituted lanthanum manganites (LNMO) were prepared by citrate gel method and characterized. These targets were laser ablated by pulsed laser deposition technique and were deposited simultaneously on silicon and relaxor ferroelectric PMN-PT substrates with a view to fabricating ferroelectric-ferromagnetic 2D heterostructures. Magnetization measurements reveal a higher magnetization for films of 100 nm thickness than the 300 nm thick films. The PMN-PT substrate influences the magnetic properties of sodium substituted lanthanum manganite thin films. The strain effects are higher for 100 nm thin films. The saturated polarization-electric field (P-E) loop measurements carried out on films demonstrated that, there is a considerable change in hysteresis parameters (coercivity and remanent polarization) upon thin film deposition. PMN-PT LNMO thin films can be viewed as a heterostructure where ferromagnetism and ferroelectricity co-exist and has potential applications in magnetoelectrics.

## 1. Introduction

Manganites have gained immense importance in the area of magnetoelectrics since they possess tunable magnetic properties (near 300 K), close correlation between lattice, charge and spin degrees of freedom and most importantly compatible crystal structure with most of the ferroelectric systems. Magnetism in these materials is mainly governed by double exchange and superexchange mechanism between mixed valence states of Mn ions with profound influence from oxygen stoichiometry, vacancy/defects and ionic radii [1–3].

Possibility of developing thin films of ferroelectric-ferromagnetic heterostructures based on lanthanum manganites (LMO) and its derivatives with a ferroelectric material gained momentum since the strain in thin films can be easily achieved by the selection of a suitable substrate and these materials are isostructural with FE materials. In bulk samples, strain is altered by ion substitution or by the application of an external hydrostatic pressure, while lattice or thermal mismatch with the substrate is sufficient for inducing strain in thin films. Such statically strained thin films are being increasingly investigated to judge the dependence of magnetic, structural and electrical properties of strain at the film-substrate interface [4–13]. Influence of epitaxial strain on magnetic parameters like Curie temperature, magnetization and anisotropy in divalent ion (like Sr and Ca) substituted LMO films (LSMO and LCMO respectively) have already been reported and attempts were also made to study the coupling nature of LSMO-BTO (Barium titanate) systems [6,7,11]. Variation in thickness was also found to have a marked influence on other factors like nature of strain, lattice structure and ferroelectric polarization. There exist vast literature on strain induced domain structure of $LaSrMnO_3$ thin films grown on BTO substrates [14], magnetocaloric effects in La(0.7)Ca(0.3)MnO(3) thin films on BTO due to strain [15], reversible biaxial strain from substrate utilized to probe the response of magnetization to strain in $SrRuO_3$ films on PMN-PT[(1-x) $Pb(Mg_{1/3}Nb_{2/3})O_3$-x$PbTiO_3$] substrates [16], magnetization switching by electric field in heterostructures of nanomagnet Co and PMN–PT [17] and resistivity changes associated with strain in epitaxial $La_{0.7}Ba_{0.3}MnO_3$ thin films [18].

* Corresponding author at: Department of Physics, Cochin University of Science and Technology, Cochin 682 022, India.
*E-mail address:* mra@cusat.ac.in (M.R. Anantharaman).
[1] Material Science and Engineering, IIT Gandhinagar, Gandhinagar 382355, Gujarat, India.
[2] Department of Materials and Earth Sciences, Technical University of Darmstadt, Karolinenpl. 5, 64289 Darmstadt, Germany.

https://doi.org/10.1016/j.jmmm.2021.168484
Received 2 December 2020; Received in revised form 28 July 2021; Accepted 25 August 2021
Available online 30 August 2021

Study on strain dependence is essential for the development of magnetoelectrics (ME) as they offer coupling between the electric and magnetic counterparts at the interface. Strain mediated ME coupling could directly unite electrical and magnetic polarizations with implications in realizing four state memory devices and spintronics [19]. In magnetoelectric composites consisting of laminated thin films of piezoelectric and magnetostrictive components, a tensile and compressive strain can lead to in-plane magnetization rotation. Such strained thin films can be obtained on substrates made from anisotropically cut piezoelectric or poled relaxor ferroelectric crystals.

Hence it would be interesting to study the nature of ferromagnetic thin films grown on strained piezoelectric substrate and the present work deals with one such heterostructure. Apart from LSMO and LCMO, which are divalent substituted manganites, monovalent substitution can be more effective in increasing the amount of charge carriers as a single monovalent ion substitution can lead to conversion of two $Mn^{3+}$ ions to $Mn^{4+}$. Such an increase in charge carrier density deeply influences the transport properties and thereby the spin dependent magnetic ordering in manganites. Monovalent ion such as sodium can be substituted for lanthanum sites in manganites since ionic radii of sodium ion (116 pm) and lanthanum ion (117.2 pm) are close to one another which limits any structural distortion of the lattice by the substitution [2,3,20].

Lanthanum manganites (LMO) with monovalent sodium substitution at La sites are chosen for the present investigation. Recently, we synthesized bulk samples of LNMO with appreciable saturation magnetization ($M_S$) and the results were very encouraging. Such a system like LNMO would be an ideal target for pulsed laser deposition (PLD) on a ferroelectric substrate like PMN-PT to form a heterostructure. The main motivation for such an investigation is to study the effects of strain on the magnetoelectric properties of the heterostructure and to study the effects of thickness of the film on the magnetic properties. Similar heterostructures on a silicon substrate was grown under identical conditions simultaneously. This enabled comparison of their properties and to study the effects of substrate if any, on the magneto-electric and electric properties.

## 2. Sample fabrication

Bulk samples of sodium substituted lanthanum manganites with 50 and 70 percent substitution of Na in La site, (LNMO5 and LNMO7) were synthesized using modified citrate gel method.

For this, stoichiometric amounts of precursors such as lanthanum oxide, manganese nitrate and sodium carbonate were dissolved in de–ionized water with an adequate amount of citric acid. Appropriate amount of nitric acid was added to the solution to convert all the constituents to nitrates and was heated at 80 °C with rigorous stirring. Upon this addition, the solution boiled, frothed, turned dark and caught fire giving a spongy dark powder which was then sintered at a temperature of 1100 °C for several hours. Structural characterization of the bulk samples indicated an orthorhombic structure with a characteristic peak at 2θ angle of 32° in *Pbnm* space group. Magnetic characterization using room temperature vibrating sample magnetometry (VSM) indicated that samples are ferromagnetic in nature with higher saturation magnetization ($M_S$) for 50 percent Na substituted sample. Detailed study on bulk samples of LNMO are described elsewhere [21].

Circular pellets of diameter 10 mm were made and these were used as the targets for PLD. PLD was chosen since thin films deposited using PLD maintains the exact stoichiometry of the target material. Pulsed laser deposition was carried out by KrF laser with a λ of 248 nm and laser fluence of 1.6 J/cm$^2$ with a repetition rate of 10 Hz. Target to substrate distance was fixed at 4.5 cm and substrate temperature of 700 °C was used. Deposition was carried out in the presence of background gas oxygen with its pressure maintained at 0.33 mbar. Thin films of LNMO5 and LNMO7 were deposited on PMN-PT [(0 0 1) plane] substrate (4 mm X 4 mm X 0.5 mm) for two different thicknesses – 100 nm and 300 nm. PMN-PT serves as a piezoelectric substrate which is also relaxor ferroelectric possessing high dielectric constant. Silicon (Si) and Chromium-gold sputtered Si substrate (Si/Cr/Au) were also placed alongside PMN-PT substrate during deposition so that thin films under identical process conditions are deposited on Si substrates too. Si substrates were chosen as it would be feasible to carry out morphological studies especially Atomic Force Microscopy (AFM) in them than on ferroelectric substrates. LNMO film deposited on Si substrates was used for structural and morphological characterizations. Deposition for other Na concentrations (in %) like 60, 80 and 90 were also carried out on Si substrates and magnetic characterization on them were utilized in the present study. But thin films of LNMO5 and LNMO7 on Si as well as on PMN-PT substrates for 100 nm and 300 nm will be the main focus of present investigation. PMN-PT substrate is gold coated on one side and the film deposition is carried out on the other side. Structural, morphological and compositional analysis was carried out using grazing incidence small-angle X-ray scattering (GISAXS), Scanning Electron Microscopy (SEM) using Hitachi S-5200 and a Philips Nova NanoSEM and equipped with EDS (Bruker) and Atomic Force Microscopy (AFM) [Veeco Dimension 3000]. Magnetic characterization of thin films was carried out using SQUID-VSM and the ferroelectric characteristics were evaluated using a Polarization-Electric field (P-E) loop tracer [Radiant Technologies].

## 3. Results and discussion

### 3.1. Structure and morphology

X-ray diffraction of bulk samples were analyzed and they exhibited an orthorhombic structure with *Pbnm* space group (refer Fig. S1, Supplementary information). The lattice parameters of the two targets after Rietveld refinement are as follows: LNMO5: a = 5.4976 Å, b = 5.4436 Å and c = 7.7385 Å; LNMO7: a = 5.4627 Å, b = 5.4121 Å and c = 7.7031 Å. It is presumed that an orthorhombic unit cell (consider $ABO_3$) is a consequence of tilting or rotations of $BO_6$ octahedra due to mismatch of *A*-O and $\sqrt{2}$(*B*-O) bonds. Thus a tilted orthorhombic unit cell can be approximated to a pseudocubic unit cell with lattice parameters [22] $a_{pseudo} \approx \frac{a}{\sqrt{2}} \approx \frac{b}{\sqrt{2}} \approx \frac{c}{2}$ and in our case, $a_{pseudo}$ is in the range of 3.8 Å for both the targets. Also, the in-plane lattice parameter of the PMN-PT (0 0 1) crystals is a = b = 4.022 Å while the Si substrate p type (1 1 0) has a lattice parameter of 5.431 Å.

Fig. 1(a) and (b) depict the XRD patterns of 300 nm LNMO5 deposited on Si (Si/LNMO5) as well as on the ferroelectric substrate, PMN-PT (PMN-PT LNMO5). The characteristic peak of perovskite structure corresponding to (1 1 0) plane is observed at 32° for both films. From the thin film XRD, out of plane lattice parameter for LNMO (1 1 0) film is about 3.9498 Å on PMN PT substrate and 3.854 Å on Si substrate which is similar to the results observed by Pomar et al. for out of plane epitaxial lanthanum manganite (1 1 0) film growth on cubic perovskite substrates. In the case of LMO and its substitutes, structural distortion of the $MnO_6$ octahedra due to Jahn teller distortion takes place. The growth of LNMO film in either (1 0 0) or (1 1 0) direction is justified to accommodate this structural distortion to the substrate/crystal [23].

SEM images of LNMO5 film deposited on Si and Si/Cr/Au substrate is shown in Fig. 1(c) and (d). The substrate and interface can be clearly visible from the image. SEM-EDS analysis from Fig. 1(e) and (g) confirms that LNMO film is stoichiometric with the ratio of La:Na as 1:1 as that of the bulk compound. SEM images of LNMO5 film deposited on PMN-PT and Si substrates are depicted in Fig. 1(g) and (h). It is inferred that a near spherical like particles overlapping each other are found on the surface of films deposited on both substrates and such surface features are more dense in PMN-PT substrate in comparison to Si substrate.

XRD and SEM studies on LNMO7 films also showed similar results. The AFM image of LNMO7 film scanned for a surface of 10 X 10 μm on Si substrate is shown here which clearly indicates spherical shaped particles with no random features in LNMO7 film (Fig. 2(a)). Fig. 2(b) depicts

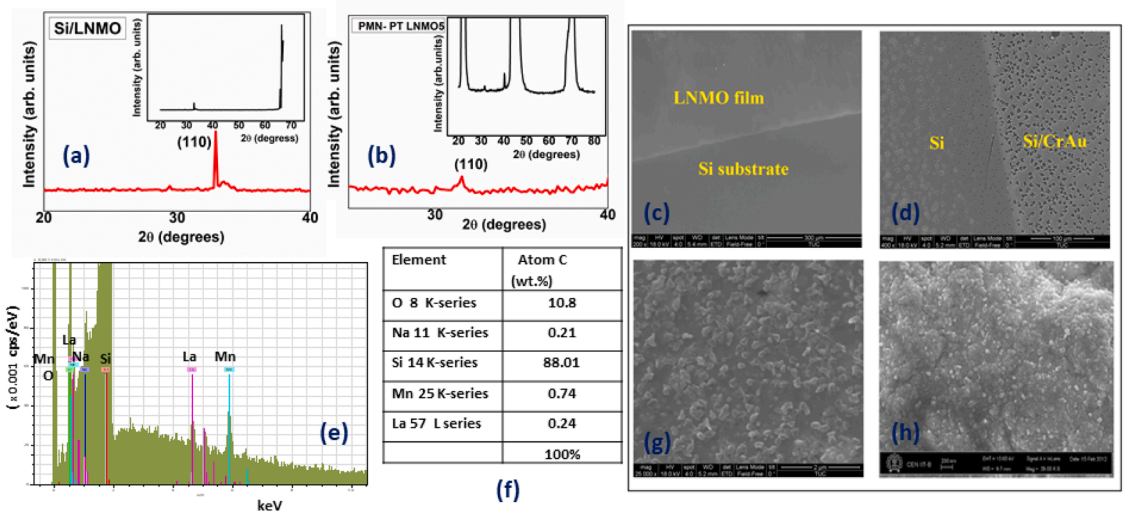


| Element | Atom C (wt.%) |
|---|---|
| O 8 K-series | 10.8 |
| Na 11 K-series | 0.21 |
| Si 14 K-series | 88.01 |
| Mn 25 K-series | 0.74 |
| La 57 L series | 0.24 |
| | 100% |

**Fig. 1.** XRD pattern of 300 nm LNMO5 film deposited on (a) Si and (b) PMN-PT substrate. SEM images of LNMO5 film from the etched/masked region showing (c) LNMO and Si interface (d) LNMO and Si/Cr/Au interface (e) SEM – EDS plot of Si/LNMO5 film showing the element peaks of La, Na, Mn, O and Si (f) Table showing the atomic wt% of each element where a near 1:1 ratio of La and Na is observed in Si/LNMO5 film. SEM images of thin films (g) Si/LNMO5 (h) PMN-PT LNMO5.

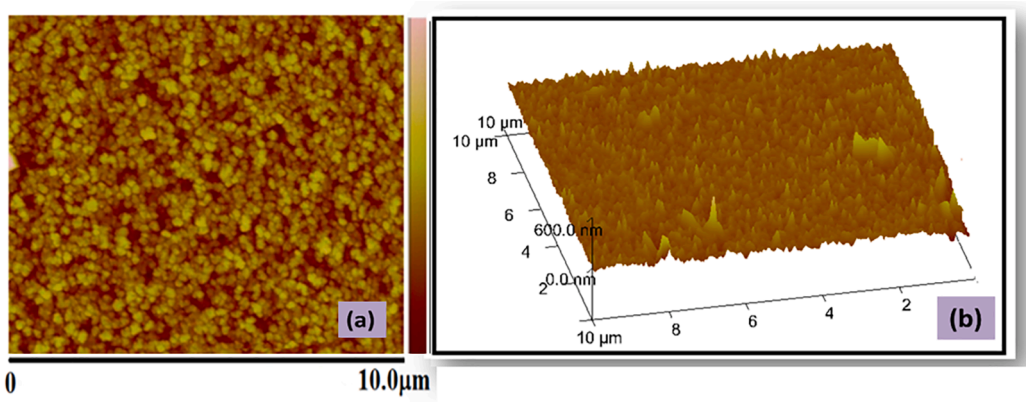


**Fig. 2.** (a) AFM images of LNMO7 film on Si substrates; (b) 3D surface topography image of LNMO7 film on Si substrate.

a 3D AFM image showing the film deposition on Si substrate. The morphology observed here follows the general morphology observed for LNMO thin films [24].

### 3.2. Magnetic characterization

Room temperature VSM measurements carried out on bulk (powder) samples of LNMO revealed that saturation magnetization ($M_S$) decreases with increase in Na concentration. Magnetization plot of bulk samples of LNMO are reproduced here for continuity (Fig. 3(a)). Fig. 3(b) presents the magnetic hysteresis (M−H) loop of LNMO films deposited on Si substrates and it is evident that in LNMO films, magnetization decreases with increase in Na concentration, like in the powder samples. Based on the observation made from Si/LNMO films, two representative samples - LNMO5 and LNMO7 were identified, as there exists a considerable difference in $M_S$ between them. The LNMO5 and LNMO7 films of two different thickness – 100 nm and 300 nm are then used for further magnetic and electrical characterization considering the economic availability of PMN-PT substrate.

Magnetic measurements on PMN-PT LNMO5 and PMN-PT LNMO7 for two different thicknesses of 300 nm and 100 nm are shown in Fig. 3 (c) and 3(d) respectively. For PMN-PT LNMO5, $M_S$ is 167 μemu/cm$^2$ for 100 nm film and 31 μemu/cm$^2$ for 300 nm thick films while for PMN-PT LNMO7, the values are 28 μemu/cm$^2$ and 10 μemu/cm$^2$ for 100 nm and 300 nm films respectively. It is observed that thinner films exhibit higher magnetization. The literature is rich especially on the effect of biaxial strain (compressive or tensile) as a control parameter in epitaxial thin films grown on crystal structure surfaces and its magnetic and transport properties [6–11]. The origin of ferromagnetic order in the manganite thin films itself is a matter of debate and has been attributed to either due to oxygen content or strain while in the case of bulk manganites, oxygen nonstoichiometry leads to octahedra distortion leading to the Jahn teller distortion and hence magnetic ordering is accountable [23]. It has been observed that in magnetic thin films, biaxial strain decreased with increase in film thickness. Thus, as thickness of films increases, the lattice relaxes while thinner films is strained in all three directions. Strained unit cell in thinner films affects magnetic properties vis-a-vis exchange interactions since they are directly linked to lattice parameters [28,29]. Such a premise is applicable to the present ferromagnetic LNMO films grown on PMN-PT substrates and the possible reason for the decrease in magnetization as the film thickness increases.

### 3.3. Ferroelectric characterization

To understand the influence of electric field or voltage on the substrate, ferroelectric hysteresis loops plotting electrical polarization, P vs Voltage were carried out as PMN-PT is also a candidate ferroelectric material. The electric leads were taken from the gold coated side and

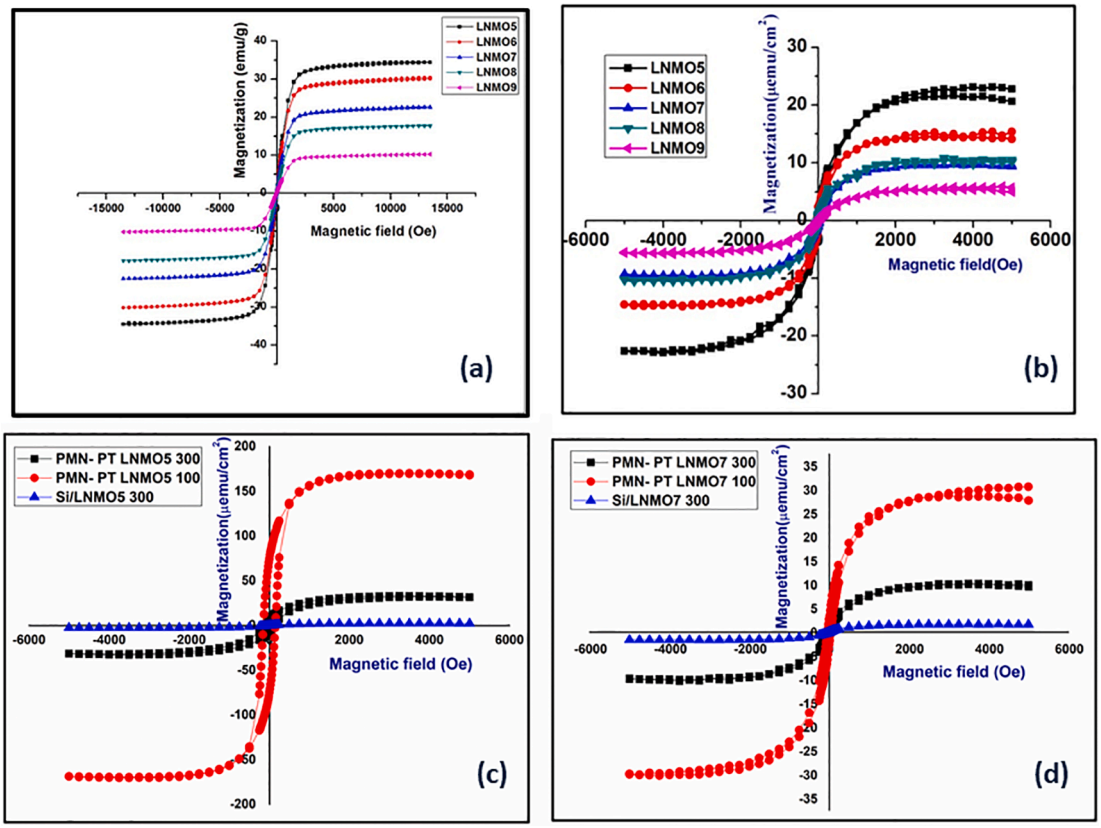


**Fig. 3.** (a) M−H loop for LNMO bulk [Reprinted from [42] Copyright (2015), with permission from Elsevier] (b) M−H loop of LNMO films deposited on Si substrate from 50 to 90 percent Na substitution denoted as LNMO5 to LNMO9. A comparative M−H loop at 300 K for (c) LNMO5 films of thickness 100 nm and 300 nm on PMN-PT and 300 nm on Si substrate (d) LNMO7 films of thickness 100 nm and 300 nm on PMN-PT and 300 nm on Si substrate.

from the LNMO film. An uncoated PMN-PT with gold coating on both sides was used as the reference. Two LNMO films - LNMO5 and LNMO7 with thickness of 100 nm were investigated and ferroelectric hysteresis loop for four different voltage ranges are recorded and depicted in Fig. 4 and Fig. S3. Polarization hysteresis is plotted with voltage on the X axis and polarization in μC/cm$^2$ on the Y axis. It is observed that in comparison to PMN-PT substrate, PMN-PT LNMO heterostructure shows an increase in coercivity ($V_C$) irrespective of the composition of films. In the case of PMN-PT LNMO5, coercivity ($V_C$) is 100.1 kV/cm, while for PMN-PT, $V_C$ is 78.7 kV/cm and on the otherhand, for PMN-PT LNMO7 it is 89.6 kV/cm. Such an increase in $V_C$ has been observed also for other 20 kV, 30 kV and 40 kV. Detailed variation of $V_C$ and remanence ($P_R$) is tabulated in Table 1. It is observed from Table 1 that coercive field change for LNMO5 is larger than LNMO7 for all the voltage ranges. In the case of LNMO7, the remanence is larger than LNMO5. It is to be noted that ferroelectric hysteresis loop of pristine LNMO bulk materials exhibited a circular loop indicative of a resistive behaviour (refer Fig. S2). Thin films on Si substrate suffered a dielectric breakdown during ferroelectric hysteresis measurement.

PMN-PT being a ferroelectric substrate, the strain can be controlled by the ferroelectric poling or converse piezoelectric effects and the induced strain in the PMN-PT will be transferred to the overlying LNMO film thereby influencing the biaxial strain of the film [30]. Thus, it could be argued that on using ferroelectric substrate, there is cumulative effect of lattice strain and tuning of strain by piezoelectric effect on application of a voltage. It has been proved in LNMO thin films that magnetoresistance/electrical transport properties of (1 1 0) oriented thin films can be tuned by different orientations of substrate than (1 0 0) oriented films [31]. Also biaxial in-plane strain relaxation on application of piezo voltage was reported in LSMO films grown on PMN-PT, where the metallic character of thin films enhanced and the ferromagnetic Curie temperature increased [32]. Variation on coercivity and remanence of ferroelectric hysteresis loops has been reported earlier in Au/BFO/LSMO/STO heterostructures and they have attributed to the epitaxial strain, interfacial layer influence and pinning of domain walls [28].

In our case, since the film growth of LNMO is in (1 1 0) direction, the lattice mismatch has to be calculated from the area of basal plane as follows: $\frac{d^2_{(110)f} - a_s^2}{a_s^2}$ where $d_{(1\,1\,0)f}$ and $a_s$ correspond to lattice parameters of film and substrate respectively. The calculated mismatch for LNMO (1 1 0) film in Si is −0.55% and in PMN PT is −0.035% which indicates that when compared to Si, growth of films on PMN PT shows better lattice matching. Since the film growth is in (1 1 0) direction, it is nearly heteroepitaxial, strain is felt in the layer so that growth of film happens coherently and the lattice changes so that in plane lattice parameters of film matches well with that of the substrate beneath [33]. The reason for growth of film in a particular direction on a substrate is not well understood, the surface energy difference between substrate and film could be one of the factors governing it. Such growth modes control the strain in films [29,34].

Thus change in coercivity and remanence in these PMN-PT LNMO films as observed from ferroelectric measurements are a result of the cumulative substrate effect of PMN-PT under the influence of applied electric field. From the magnetic and ferroelectric hysteresis results and based on existing literature, it is assumed that strain could be one influencing factor [25–27]. Magnetic measurements already proved that LNMO7 is less magnetic than LNMO5 and possibly strain/stress could be in a relaxed state compared to LNMO5 causing an enhancement of remanent polarization as observed earlier in BFO films [34]. The strain/stress influence on LNMO5 films is larger which could have caused an increase in coercivity in agreement with earlier reports on ferroelectric substrates [9,10].

The strain/stress influence in these PMN PT LNMO system is a first

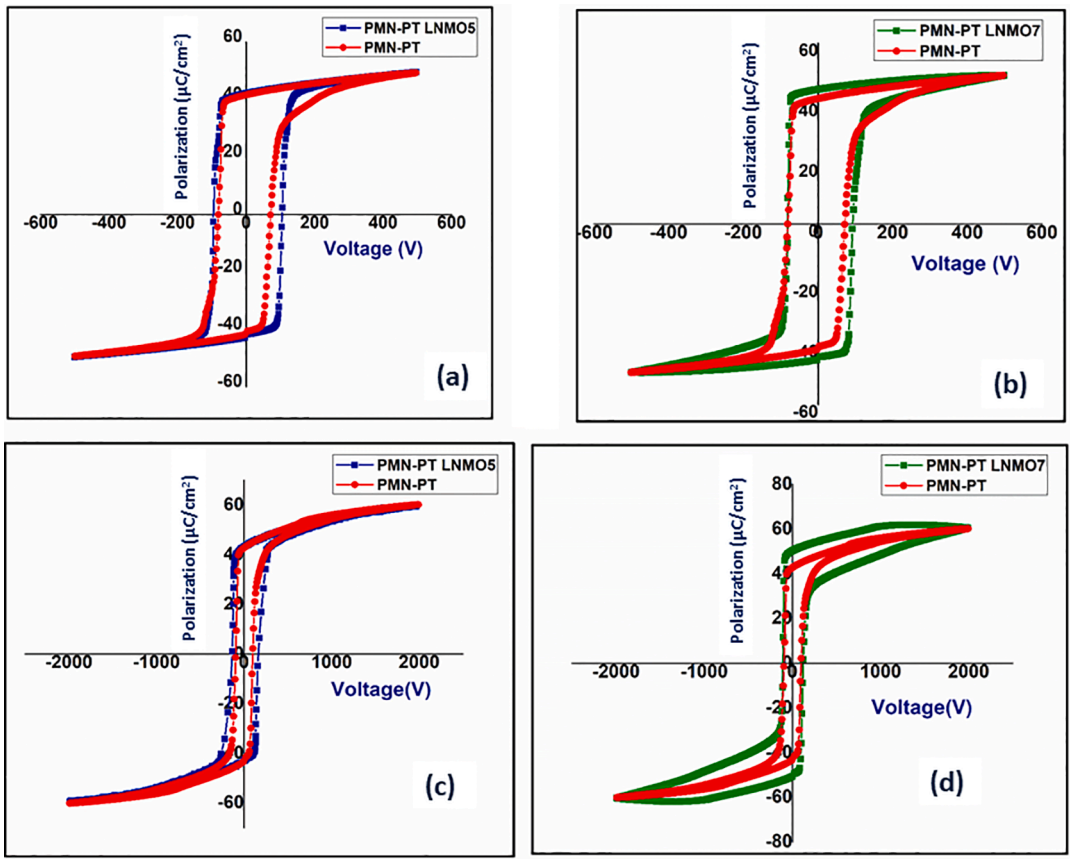


**Fig. 4.** (a) and (b) Polarization hysteresis on PMN-PT LNMO5 and PMN-PT LNMO7 films (100 nm) respectively in comparison to PMN-PT substrates for voltage ($V_{max}$) upto 500 V. (c) and (d) Polarization hysteresis on PMN-PT LNMO5 and PMN-PT LNMO7 films (100 nm) respectively in comparison to PMN-PT substrates for voltage ($V_{max}$) upto 2000 V.

**Table 1**
Table showing parameters like Coercivity ($V_C$), Remanent ($P_R$) and Saturation polarization ($P_S$) for LNMO5 and LNMO7 films from ferroelectric hysteresis measurements.

| $V_{max}$ | 500 V | | | 1000 V | | | 1500 V | | | 2000 V | | |
|---|---|---|---|---|---|---|---|---|---|---|---|---|
| SAMPLE CODE | $V_C$ (V) | $P_R$ ($\mu C/cm^2$) | $P_S$ | $V_C$ (V) | $P_R$ ($\mu C/cm^2$) | $P_S$ | $V_C$ (V) | $P_R$ ($\mu C/cm^2$) | $P_S$ | $V_C$ (V) | $P_R$ ($\mu C/cm^2$) | $P_S$ |
| PMN-PT | 78.7 | 41.6 | 48.1 | 80.5 | 42.2 | 54.5 | 85.4 | 42.5 | 57.6 | 98.3 | 42.2 | 59.6 |
| PMN-PT LNMO5 | 100.1 | 42.17 | 49.2 | 110.6 | 42.7 | 55.1 | 118 | 43.1 | 57.9 | 145.9 | 43.1 | 59.7 |
| PMN-PT LNMO7 | 89.6 | 44.6 | 49.2 | 92.6 | 47.1 | 55.1 | 103.8 | 48.9 | 59.1 | 114.3 | 50.2 | 61.3 |

hand information drawn from the magnetic/ferroelectric measurements. It is also necessary to further analyze heteroepiaxy as well as composition gradient of films and coupling behaviour of FE and FM orders.

## 4. Conclusion

Sodium substituted lanthanum manganite (LNMO) films were deposited on ferroelectric PMN-PT substrates with the aim of developing a ferroelectric – ferromagnetic heteroepitaxial structure. Sodium substitution at the lanthanum site (50 and 70 percent) were carried out in lanthanum manganites and the thin films were deposited by PLD on Si and relaxor ferroelectric PMN-PT substrate. Thin films on PMN-PT substrate demonstrated higher magnetization for 100 nm films in comparison to 300 nm films, which indicated that substrate strain of PMN-PT changes the Mn-O-Mn bond length and bond angles of LNMO responsible for magnetism in manganites; the strain effects are higher for thinner films. Polarization hysteresis measurements carried out on LNMO5 and LNMO7 films demonstrated that there is a considerable change in $V_C$ and $P_R$ of PMN-PT substrate upon thin film deposition.

## 5. Author statement

N.S. has carried out the synthesis and analysis under the supervision of M.R.A and G.S. N.S. and L.K.V carried out the ferroelectric measurements and analysis. N.S and S.T carried out the magnetic measurements and analysis. M.R.A and N.S. contributed in conceptualizing, writing and design of work. All the authors contributed in finalizing the manuscript.

## Declaration of Competing Interest

The authors declare that they have no known competing financial interests or personal relationships that could have appeared to influence the work reported in this paper.

## Acknowledgements

N.S acknowledges DST INSPIRE fellowship (No. DST/INSPIRE Fellowship/2010/236) and DST WoS-A project (No. SR/WOS-A/PM-35/2017(G)). M.R.A acknowledges BRNS Project No. 2011/34/7/BRNS/0596. M.R.A also acknowledges University Grants Commission, Government of India for awarding UGC-BSR faculty fellowship (No. F.18-1/2011(BSR) dated 04/01/2017). N.S and M.R.A are grateful to INUP programme of CEN, IIT- Bombay and DST DAAD PPP programme. N.S also extends gratitude to Prof. Manfred Albrecht, Dr. Andreas Leibig, University of Augsburg, Germany and Prof. Rajeev Ranjan, Department of Materials Engineering, Indian Institute of Science, Bangalore. S. Thomas kindly acknowledges the financial support from DST, New Delhi via INSPIRE Faculty award.

## Appendix A. Supplementary data

Supplementary data to this article can be found online at https://doi.org/10.1016/j.jmmm.2021.168484.

## References

[1] M.B. Salamon, M. Jaime, Rev. Mod. Phys. 73 (2001) 583.
[2] S. Roy, Y.Q. Guo, S. Venkatesh, N. Ali, J. Phys.: Condens. Matter 13 (2001) 9547.
[3] A. Das, M. Sahana, S.M. Yusuf, L.M. Rao, C. Shivakumara, M.S. Hegde, Mater. Res. Bull. 35 (2000) 651.
[4] B. Özkaya, S.R. Saranu, S. Mohanan, U. Herr, Physica Status Solidi (a) 205 (2008) 1876.
[5] R.V. Chopdekar, V.K. Malik, A. Fraile Rodríguez, L. Le Guyader, Y. Takamura, A. Scholl, D. Stender, C.W. Schneider, C. Bernhard, F. Nolting, L.J. Heyderman, Phys. Rev. B 86 (2012), 014408.
[6] K. Dörr, O. Bilani-Zeneli, A. Herklotz, A.D. Rata, K. Boldyreva, J.-W. Kim, M. C. Dekker, K. Nenkov, L. Schultz, M. Reibold, Eur. Phys. J. B 71 (2009) 361.
[7] S.A. Solopan, O.I. V'yunov, A.I. Tovstolytkin, L.L. Kovalenko, A.G. Belous, Inorg. Mater. 43 (2007) 1252.
[8] V. Peña, Z. Sefrioui, D. Arias, C. León, J. Santamaria, M. Varela, S.J. Pennycook, M. Garcia-Hernandez, J.L. Martinez, J. Phys. Chem. Solids 67 (2006) 472.
[9] S. Sakuragi, T. Sakai, S. Urata, S. Aihara, A. Shinto, H. Kageshima, M. Sawada, H. Namatame, M. Taniguchi, T. Sato, Phys. Rev. B 90 (2014), 054411.
[10] J. Cao, J. Wu, Mater. Sci. Eng.: R: Rep. 71 (2011) 35.
[11] H. Boschker, J. Kautz, E.P. Houwman, W. Siemons, D.H.A. Blank, M. Huijben, G. Koster, A. Vailionis, G. Rijnders, Phys. Rev. Lett. 109 (2012), 157207.
[12] O. Shapoval, S. Hühn, J. Verbeeck, M. Jungbauer, A. Belenchuk, V. Moshnyaga, J. Appl. Phys. 113 (2013) 17C711.
[13] M.G. Praveena, A.S. Kumar, M.S. Kala, R.N. Bhowmik, S. Swapna, Thomas, S. Nair, M.R. Anantharaman, J. Magn. Magn. Mater. 513 (2020), 167252.
[14] R.V. Chopdekar, J. Heidler, C. Piamonteze, Y. Takamura, A. Scholl, S. Rusponi, H. Brune, L.J. Heyderman, F. Nolting, Eur. Phys. J. B 86 (2013) 241.
[15] X. Moya, L.E. Hueso, F. Maccherozzi, A.I. Tovstolytkin, D.I. Podyalovskii, C. Ducati, L.C. Phillips, M. Ghidini, O. Hovorka, A. Berger, M.E. Vickers, E. Defay, S.S. Dhesi, N.D. Mathur, Nat. Mater. 12 (2013) 52.
[16] A. Herklotz, M. Kataja, K. Nenkov, M.D. Biegalski, H.-M. Christen, C. Deneke, L. Schultz, K. Dörr, Phys. Rev. B 88 (2013), 144412.
[17] M. Yi, B.-X. Xu, R. Müller, D. Gross, Acta Mech. 230 (2019) 1247.
[18] G.A. Ovsyannikov, T.A. Shaikhulov, V.A. Shakhunov, V.L. Preobrazhensky, T. Mathurin, N. Tiercelin, P. Pernod, J. Supercond. Nov. Magn. 32 (2019) 2759.
[19] W. Eerenstein, N.D. Mathur, J.F. Scott, Nature 442 (2006) 759.
[20] C. Aruta, M. Angeloni, G. Balestrino, N.G. Boggio, P.G. Medaglia, A. Tebano, B. Davidson, M. Baldini, D. Di Castro, P. Postorino, P. Dore, A. Sidorenko, G. Allodi, R. De Renzi, J. Appl. Phys. 100 (2006), 023910.
[21] N. Sethulakshmi, A.N. Unnimaya, I.A. Al-Omari, S. Al-Harthi, S. Sagar, S. Thomas, G. Srinivasan, M.R. Anantharaman, J. Magn. Magn. Mater. 391 (2015) 75.
[22] A. Vailionis, H. Boschker, W. Siemons, E.P. Houwman, D.H.A. Blank, G. Rijnders, G. Koster, Phys. Rev. B 83 (2011), 064101.
[23] A. Pomar, Z. Konstantinović, N. Bagués, J. Roqueta, L. López-Mir, L. Balcells, C. Frontera, N. Mestres, A. Gutiérrez-Llorente, M. Šćepanović, N. Lazarević, Z. V. Popović, F. Sandiumenge, B. Martínez, J. Santiso, Front. Phys. (2016).
[24] L. Malavasi, M.C. Mozzati, I. Alessandri, M. Affronte, V. Cervetto, C.B. Azzoni, G. Flor, Solid State Ionics 172 (2004) 265.
[25] T. Liu, C.S. Lynch, Acta Mater. 51 (2003) 407.
[26] A.I. Tovstolytkin, A.M. Pogorily, S.A. Solopan, O.I. V'Yunov, L.L. Kovalenko, A.G. Belous, Ukr. J. Phys. 53, 4 (n.d.).
[27] J. (崔继斋) Cui, J.L. Hockel, P.K. Nordeen, D.M. Pisani, C. Liang, G.P. Carman, C. S. Lynch, Appl. Phys. Lett. 103 (2013) 232905.
[28] L. Wang, Z. Wang, K. Jin, J. Li, H. Yang, C. Wang, R. Zhao, H. Lu, H. Guo, G. Yang, Appl. Phys. Lett. 102 (2013), 242902.
[29] M. Pathak, H. Sato, X. Zhang, K.B. Chetry, D. Mazumdar, P. LeClair, A. Gupta, J. Appl. Phys. 108 (2010), 053713.
[30] R.K. Zheng, H.-U. Habermeier, H.L.W. Chan, C.L. Choy, H.S. Luo, Phys. Rev. B 81 (2010), 104427.
[31] I. Alessandri, L. Malavasi, E. Bontempi, M.C. Mozzati, C.B. Azzoni, G. Flor, L. E. Depero, Mater. Sci. Eng., B 109 (2004) 203.
[32] C. Thiele, K. Dörr, S. Fähler, L. Schultz, D.C. Meyer, A.A. Levin, P. Paufler, Appl. Phys. Lett. 87 (2005), 262502.
[33] A. Vailionis, W. Siemons, G. Koster, Appl. Phys. Lett. 93 (2008), 051909.
[34] Y. Wang, M. Zhang, E.I. Meletis, Coatings 5 (2015) 802.